Signatures for a Classical to Quantum Transition of a Driven Nonlinear Nanomechanical Resonator

Itamar Katz, Alex Retzker,* Raphael Straub,† and Ron Lifshitz‡

School of Physics & Astronomy, Raymond and Beverly Sackler Faculty of Exact Sciences, Tel Aviv University, Tel Aviv 69978, Israel

(Received 11 February 2007; published 26 July 2007)

We seek the first indications that a nanoelectromechanical system (NEMS) is entering the quantum domain as its mass and temperature are decreased. We find them by studying the transition from classical to quantum behavior of a driven nonlinear Duffing resonator. Numerical solutions of the equations of motion, operating in the bistable regime of the resonator, demonstrate that the quantum Wigner function gradually deviates from the corresponding classical phase-space probability density. These clear differences that develop due to nonlinearity can serve as experimental signatures, in the near future, that NEMS resonators are entering the quantum domain.

DOI: 10.1103/PhysRevLett.99.040404 PACS numbers: 03.65.Ta, 03.65.Yz, 05.45.−a, 85.85.+j

The race to observe quantum-mechanical behavior in human-made nanoelectromechanical systems (NEMS) is bringing us closer than ever to testing the basic principles of quantum mechanics [1,2]. With recent experiments coming within just an order of magnitude from the ability to observe quantum zero-point motion [3–5], ideas about the quantum-to-classical transition [6–8] may soon become experimentally accessible, more than 70 years after Schrödinger described his famous cat paradox [9]. As nanomechanical resonators become smaller, their masses decrease and natural frequencies Ω increase—exceeding 1 GHz in recent experiments [10,11]. For such frequencies it is sufficient to cool down to temperatures on the order of 50 mK for the quantum energy $\hbar\Omega$ to be comparable to the thermal energy $k_B T$. Such temperatures should allow one to observe truly quantum-mechanical phenomena, such as resonances, oscillator number states, superpositions, and entanglement [12–16], at least for macroscopic objects that are sufficiently isolated from their environment.

In this Letter we seek the first experimental signatures, indicating that a mechanical object is entering the quantum domain as its mass and temperature are decreased. Are there any clear quantum-mechanical corrections to classical dynamics that we can hope to observe even before the fully quantum regime is accessible experimentally? To answer this question we perform two separate calculations on the same physical object—a driven nanomechanical resonator—viewing it once as a quantum-mechanical system and once as a classical system. With everything else being equal, this allows us to contrast the dynamics of a classical resonator with that of its quantum clone. We can then search for a regime in which quantum dynamics just begins to deviate away from classical dynamics, providing us with the experimental signatures we are looking for.

We calculate the dynamics numerically. We start each quantum calculation with a coherent state, which is a minimal wave packet centered about some point in phase space. We start the corresponding classical calculation with an ensemble of initial conditions—typically of $N = 10^4$ points—drawn from a Gaussian distribution in phase space that is identical to the initial quantum-mechanical probability density. As done previously in similar situations [17], we display the calculated quantum dynamics in phase space using the quantum Wigner function

$$W(x, p, t) = \frac{1}{\pi\hbar}\int_{-\infty}^{\infty} dx' e^{-(2i/\hbar)px'}\langle x + x'|\rho(t)|x - x'\rangle, \tag{1}$$

where $\rho(t)$ is the density operator, and compare it with the time evolution of the classical phase-space density. We remind the reader that the Wigner function is not a true probability distribution as it may possess negative values, particularly when the quantum state has no classical analog. Nevertheless, its governing equation of motion reduces to the classical Liouville equation upon formally setting $\hbar = 0$, or whenever the potential is no more than quadratic. Moreover, it reduces to the quantum probability $P(x, t)$ of observing the system at position x at time t upon integration over p, and vice versa.

We perform our calculations for three qualitatively different situations: (i) An isolated resonator with no coupling to the environment; (ii) a resonator coupled to a heat bath at temperature $T_{\text{env}} = 0$; and (iii) a resonator coupled to a heat bath at a finite temperature $T_{\text{env}} > 0$. In all cases we expect to find a regime in which the evolution of quantum observables agrees with the corresponding classical averages at least up to the so-called "Ehrenfest time" [18,19], although it is generally difficult to strictly define this time scale [20,21]. For the isolated resonator, we do not expect to see a convergence of the two phase-space distributions, as the limit of $\hbar \to 0$ is singular [22,23]. When we couple the resonator to an environment, as in a real experiment, we do expect to see a gradual classical to quantum transition [23–25]. We wish to study the details of this transition.

As mentioned above, the quantum dynamics of a coherent state in a harmonic potential is essentially classical. We therefore consider a driven Duffing resonator—a nonlinear resonator commonly observed in experiments [26–29],

whose Hamiltonian is given by

$$H_{\rm sys} = \tfrac{1}{2}p^2 + \tfrac{1}{2}x^2 - xF\cos\omega t + \tfrac{1}{4}\varepsilon x^4, \qquad (2)$$

where the mass m of the resonator, and its natural frequency Ω have been scaled to 1 by an appropriate choice of units. Thus, we measure the degree in which we approach the quantum domain by an increasing effective value of $\hbar$, as measured in the scaled units. We shall reinterpret these values later in terms of real experimental masses and frequencies. The remaining parameters in the Hamiltonian are the driving amplitude F, the driving frequency ω, and the nonlinearity parameter ε. For the calculations presented here we take $\varepsilon = 0.01$, $F = 0.015 - 0.06$, and $\omega = 1.016 - 1.02$. For this choice of parameters the classical Duffing resonator is in the bistability regime, where in the presence of dissipation it can oscillate at one of two different amplitudes, depending on its initial conditions.

For the isolated quantum resonator we integrate the Schrödinger equation numerically by expanding the wave function in a truncated harmonic-oscillator energy basis $|n\rangle$. From the wave function we calculate the Wigner function (1), and compare it to the integrated classical trajectories of the corresponding Gaussian distribution of initial conditions. Figure 1 shows the two distributions, calculated for $\hbar = 0.2$, and scaled to a power of $\frac{1}{4}$ to enhance weak features, where blue (dark gray) denotes positive values, and red (light gray) denotes negative values.

We clearly see similarities between the quantum and the classical distributions, namely, the positive backbone of the Wigner function which resembles the classical distribution for short times, and the maxima of the two distributions, which are roughly in the same positions in phase space. Nevertheless, two differences prevent the distributions from approaching each other even in the limit of $\hbar \to 0$. These are the strong interference pattern in the Wigner function and the infinitely fine structure that develops in the classical distribution. As noted by Berry [22], the only

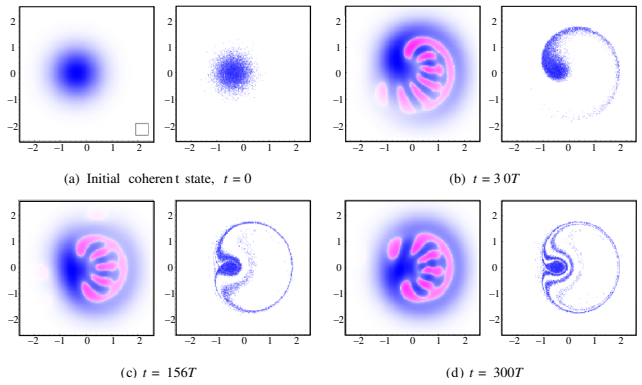

FIG. 1 (color online). Isolated driven Duffing resonator with $\hbar = 0.2$. Wigner functions (left) and classical distributions (right) of the initial coherent state and its evolution at three later times, where $T = 2\pi/\omega$. A square of area $\hbar$ is shown at the bottom right corner of (a). Full animation can be downloaded from [30].

way to obtain a smooth transition from classical to quantum dynamics in this case is to perform some averaging over a finite phase-space area $\Delta x \Delta p \simeq \hbar$, taking into account the limited precision of typical measurement devices. Such averaging will smooth out the delicate structure in the classical phase-space density and will cancel out the interference fringes in the quantum Wigner function, bringing the two into coincidence.

Next we consider the influence of an environment. For the classical resonator we use a standard Langevin approach, adding a velocity dependent dissipative term $-\gamma\dot{x}$ and a time dependent random force $\delta F(t)$. The latter is assumed to be a δ-correlated Gaussian white noise, related to the dissipative term according to the fluctuation-dissipation theorem, thus defining a temperature $T_{\rm env}$. The quantum resonator is coupled linearly to a bath of simple harmonic oscillators in thermal equilibrium at temperature $T_{\rm env}$. This adds two terms to the quantum Hamiltonian (2)—a Hamiltonian for the bath $H_{\rm bath}$, and a standard interaction Hamiltonian [15], taken to be of the Caldeira-Leggett [31] type in the rotating-wave approximation,

$$H_{\rm int} = \sum_i (\kappa_i b_i a^\dagger + \kappa_i^* b_i^\dagger a), \qquad (3)$$

where the κ_i are bilinear coupling constants, the b_i are annihilation operators acting on the bath oscillators, and a is the annihilation operator of the Duffing resonator.

We consider the reduced density operator $\rho_{\rm sys}$ of the Duffing resonator by tracing over the bath degrees of freedom. By assuming the interaction to be weak, and by employing the Markov approximation which assumes the bath has no memory, we obtain a standard master equation [15,32,33],

$$\begin{aligned}\dot{\rho}_{\rm sys} = {} & \frac{1}{i\hbar}[H_{\rm sys}, \rho_{\rm sys}] \\ & - \frac{\gamma}{2}(1+\bar{n})(a^\dagger a\rho_{\rm sys} + \rho_{\rm sys}a^\dagger a - 2a\rho_{\rm sys}a^\dagger) \\ & - \frac{\gamma}{2}\bar{n}(aa^\dagger\rho_{\rm sys} + \rho_{\rm sys}aa^\dagger - 2a^\dagger\rho_{\rm sys}a), \end{aligned} \qquad (4)$$

where $\bar{n} = (e^{\hbar\Omega/k_B T_{\rm env}} - 1)^{-1}$ is the Bose-Einstein mean occupation, $\gamma = 2\pi g(\Omega)|\kappa(\Omega)|^2$ is interpreted as the damping constant, and $g(\Omega)$ and $\kappa(\Omega)$ are the density of states of the bath and the coupling strength, respectively, both evaluated at the natural frequency $\Omega = 1$ of the resonator, because the nonlinearity is small. Instead of integrating (4) directly, we use the Monte Carlo wave function method [34,35], which is more efficient computationally.

Figure 2 shows the calculated results for a Duffing resonator with $\hbar = 0.1$, coupled to a heat bath at temperature $T_{\rm env} = 0$. We take the initial state to be centered around a point in phase space that under classical dissipative dynamics flows towards the state of large amplitude oscillations. At short times we see a general positive outline of the Wigner function which is similar to the classical density, but it quickly deviates from the classical distribu-

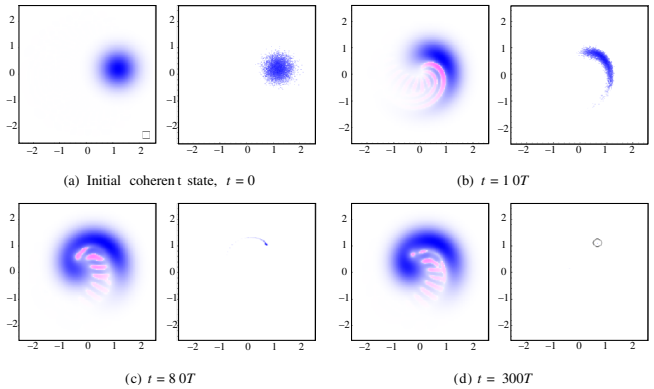

FIG. 2 (color online). As in Fig. 1, but for a driven Duffing resonator with $\hbar = 0.1$, coupled to a heat bath at $T_{\mathrm{env}} = 0$, with damping constant $\gamma = 0.01$. The stable solution towards which all initial classical points flow is encircled in (d). Full animation can be downloaded from [30].

tion. The uncertainly principle prevents it from shrinking to a point as in the classical dynamics. More importantly, we clearly observe that the Wigner distribution has substantial weight around the state of small-amplitude oscillations, which is inaccessible classically for the chosen initial conditions at $T_{\mathrm{env}} = 0$. The quantum resonator can switch between the two stable states via tunneling—in analogy with the macroscopic quantum tunneling between two equilibrium states of a static system [13]—or quantum activation [36,37], although at this point it is impossible for us to distinguish between these two processes.

Figure 3 shows the calculated results for a Duffing resonator with $\hbar = 0.1$, coupled to a heat bath at a finite temperature $k_B T_{\mathrm{env}} = 2\hbar\Omega$. This temperature is obtained by adding a fluctuating force while reducing the dissipation, thus requiring a longer time for the resonator to reach its final steady state. Here we choose the initial state to straddle the separatrix between regions in phase space that flow to the two stable states. The interference pattern that develops for short times within the general positive outline

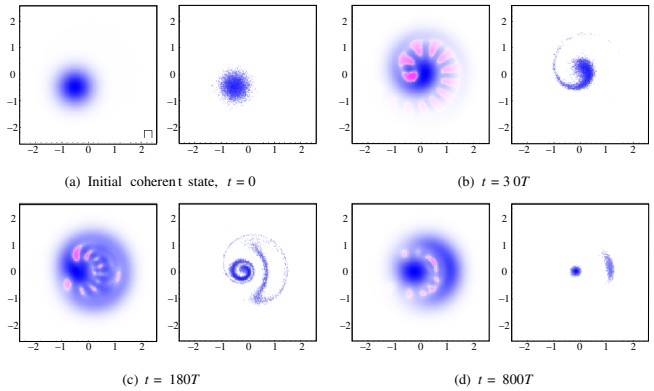

FIG. 3 (color online). As in Fig. 1, but for a driven Duffing resonator with $\hbar = 0.1$, coupled to a heat bath at $k_B T_{\mathrm{env}} = 2\hbar\Omega$, with damping constant $\gamma = 0.001$. The initial state is centered on the separatrix so that classically it splits towards both of the stable solutions. Full animation can be downloaded from [30].

in the Wigner function is soon destroyed by decoherence, and becomes erratic in space and time. At long times, both distributions peak around the two stable states, nevertheless they differ significantly. The classical density is tightly localized around the two solutions with no overlap, indicating that T_{env} is too small to induce thermal switching between the states, as was observed in a recent experiment [29]. The Wigner function, on the other hand, is spread out in phase space, indicating that $\hbar$ is sufficiently large for the quantum resonator to switch between the two states. This is demonstrated more clearly in Fig. 4, which shows the probability distributions $P(x)$ at the steady state. We find that only for temperatures as high as $k_B T_{\mathrm{env}} = 17\hbar\Omega$ does the classical phase-space distribution become as wide as the Wigner function is at $k_B T_{\mathrm{env}} = 2\hbar\Omega$, as shown in Fig. 5. Thus, in a real experiment, evidence for quantum-mechanical dynamics can be demonstrated as long as temperature and other sources of noise can be controlled to better than an order of magnitude.

We have found the signatures we were seeking for a mechanical system entering the quantum domain with effective $\hbar = 0.1$ and $k_B T_{\mathrm{env}} = 2\hbar\Omega$. They stem from the ability of a quantum Duffing resonator to switch between the two stable states, having finite probability of being in between the two states, while the classical resonator cannot. We intend to study individual quantum trajectories of the resonator to determine whether switching takes place via tunneling or quantum activation [36,37].

An effective $\hbar \simeq 0.1$ implies that the area in phase space where the dynamics takes place, is on the order of $10\hbar$. This area is roughly $x_{\max} p_{\max} \simeq m\Omega a_c^2$, where a_c—the critical oscillation amplitude for the onset of bistability—is proportional to $d/\sqrt{Q}$ [27], with d being the diameter of the resonator, and Q its quality factor. In current NEMS resonators [27,28] $m \simeq 10^{-18}$ kg, $\Omega \simeq 10^8$ Hz, and $a_c \simeq 10^{-9}$ m, yielding an effective $\hbar$ of 10^{-6}, which is well within the classical domain. Yet, if we consider suspended nanotubes [38,39], then optimistic values may give $m \simeq 10^{-21}$ kg, $\Omega \simeq 10^8$ Hz, and $a_c \simeq 10^{-11}$ m, for which the effective $\hbar \simeq 10$, which is much better than needed, while requiring a temperature of $T_{\mathrm{env}} \simeq 10$ mK. We therefore believe that it should be possible to realize our calculations in a real experiment in the near future. We should also note that since our calculations are quite general, one may be able to realize them in other

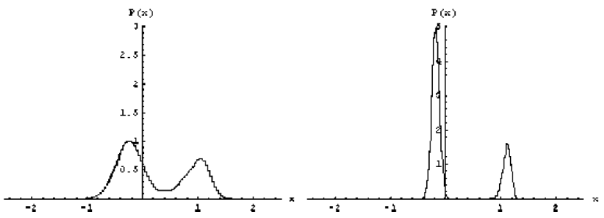

FIG. 4. Quantum (left) and classical (right) probability densities $P(x)$ for the phase-space distributions in Fig. 3(d). The y axes are scaled differently for better visualization.

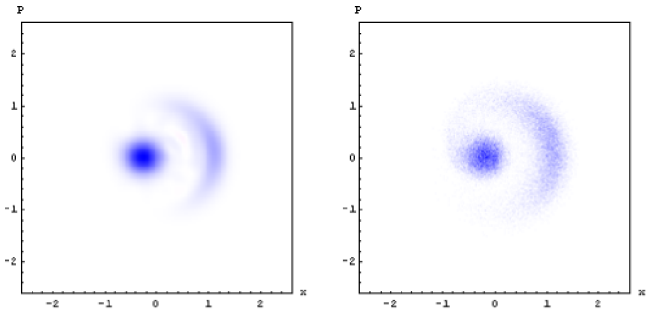

(a) Phase spaced ensities, $t = 800T$

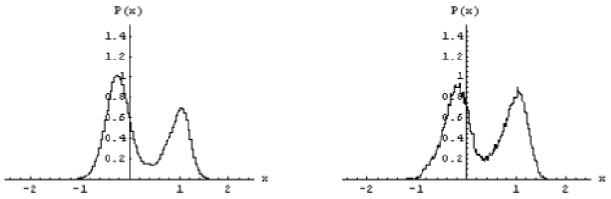

(b) Probability densities $P(x)$at $t = 800T$

FIG. 5 (color online). As in Figs. 3(d) and 4, only that the classical calculation (right) is for $k_B T_{\mathrm{env}} = 17\hbar\Omega$, yielding similar phase-space distributions (a) and probability densities (b). Both distributions in (a) are left unscaled.

nonlinear physical systems such as the SQUID, in which superpositions of distinct macroscopic states have already been demonstrated [40,41].

The authors thank Michael Cross, Mark Dykman, Jens Eisert, Victor Fleurov, Inna Kozinsky, Michael Roukes, and Keith Schwab for illuminating discussions. R. S. is grateful to the Lion Foundation for supporting his stay at Tel Aviv University as an exchange student. This research is supported by the U.S.–Israel Binational Science Foundation under Grant No. 2004339, and by the Israeli Ministry of Science.

*Current address: Institute for Mathematical Sciences, Imperial College London, SW7 2PE, U.K.
†Permanent address: Department of Physics, University of Konstanz, D-78457 Konstanz, Germany.
‡Corresponding author.
ronlif@tau.ac.il

[1] M. P. Blencowe, Phys. Rep. **395**, 159 (2004).
[2] K. C. Schwab and M. L. Roukes, Phys. Today **58**, No. 7, 36 (2005).
[3] R. G. Knobel and A. N. Cleland, Nature (London) **424**, 291 (2003).
[4] M. D. LaHaye, O. Buu, B. Camarota, and K. C. Schwab, Science **304**, 74 (2004).
[5] A. Naik, O. Buu, M. D. LaHaye, A. D. Armour, A. A. Clerk, M. P. Blencowe, and K. C. Schwab, Nature (London) **443**, 193 (2006).
[6] R. Penrose, Gen. Relativ. Gravit. **28**, 581 (1996).
[7] A. J. Leggett, J. Supercond. **12**, 683 (1999).
[8] A. J. Leggett, J. Phys. Condens. Matter **14**, R415 (2002).
[9] E. Schrödinger, Naturwissenschaften **23**, 807 (1935).
[10] X. M. H. Huang, C. A. Zorman, M. Mehregany, and M. L. Roukes, Nature (London) **421**, 496 (2003).
[11] A. N. Cleland and M. R. Geller, Phys. Rev. Lett. **93**, 070501 (2004).
[12] V. Peano and M. Thorwart, Phys. Rev. B **70**, 235401 (2004).
[13] S. M. Carr, W. E. Lawrence, and M. N. Wybourne, Phys. Rev. B **64**, 220101(R) (2001).
[14] A. D. Armour, M. P. Blencowe, and K. C. Schwab, Phys. Rev. Lett. **88**, 148301 (2002).
[15] D. H. Santamore, A. C. Doherty, and M. C. Cross, Phys. Rev. B **70**, 144301 (2004).
[16] J. Eisert, M. B. Plenio, S. Bose, and J. Hartley, Phys. Rev. Lett. **93**, 190402 (2004).
[17] T. Novotńy, A. Donarini, and A.-P. Jauho, Phys. Rev. Lett. **90**, 256801 (2003).
[18] M. V. Berry and N. L. Balazs, J. Phys. A **12**, 625 (1979).
[19] F. Cametti and C. Presilla, Phys. Rev. Lett. **89**, 040403 (2002).
[20] A. C. Oliveira, M. C. Nemes, and K. M. Fonseca Romero, Phys. Rev. E **68**, 036214 (2003).
[21] A. C. Oliveira, J. G. Peixoto de Faria, and M. C. Nemes, Phys. Rev. E **73**, 046207 (2006).
[22] M. V. Berry, *Chaos and Quantumphysics* (Elsevier, New York, 1991), Chap. 4.
[23] S. Habib, K. Jacobs, H. Mabuchi, R. Ryne, K. Shizume, and B. Sundaram, Phys. Rev. Lett. **88**, 040402 (2002).
[24] B. D. Greenbaum, S. Habib, K. Shizume, and B. Sundaram, Chaos **15**, 033302 (2005).
[25] S. Habib *et al.*, arXiv:quant-ph/0505046.
[26] H. G. Craighead, Science **290**, 1532 (2000).
[27] H. W. C. Postma, I. Kozinsky, A. Husain, and M. L. Roukes, Appl. Phys. Lett. **86**, 223105 (2005).
[28] I. Kozinsky, H. W. C. Postma, I. Bargatin, and M. L. Roukes, Appl. Phys. Lett. **88**, 253101 (2006).
[29] J. S. Aldridge and A. N. Cleland, Phys. Rev. Lett. **94**, 156403 (2005).
[30] See EPAPS Document No. E-PRLTAO-99-075729 for full animations of phase space distributions and probability densities corresponding to Figs. 1–3. For more information on EPAPS, see http://www.aip.org/pubservs/epaps.html.
[31] A. O. Caldeira and A. J. Leggett, Ann. Phys. (N.Y.) **149**, 374 (1983).
[32] W. Louisell, *Quantum Statistical Properties of Radiation* (John Wiley & Sons, New York, 1973).
[33] C. W. Gardiner and P. Zoller, *Quantum Noise* (Springer, Berlin, 2004), 3rd ed.
[34] K. Mølmer, Y. Castin, and J. Dalibard, J. Opt. Soc. Am. B **10**, 524 (1993).
[35] M. B. Plenio and P. L. Knight, Rev. Mod. Phys. **70**, 101 (1998).
[36] M. Marthaler and M. I. Dykman, Phys. Rev. A **73**, 042108 (2006).
[37] M. I. Dykman, Phys. Rev. E **75**, 011101 (2007).
[38] V. Sazonova, Y. Yaish, H. Üstünel, D. Roundy, T. A. Arias, and P. L. McEuan, Nature (London) **431**, 284 (2004).
[39] B. Witkamp, M. Poot, and H. S. J. van derZant, Nano Lett. **6**, 2904 (2006).
[40] J. R. Friedman, V. Patel, W. Chen, S. K. Tolpygo, and J. E. Lukens, Nature (London) **406**, 43 (2000).
[41] A. Lupascu *et al.*, Nature Phys. **3**, 119 (2007).